Scripta METALLURGICA Vol. 12, pp. 21-26, 1978 Pergamon Press, Inc.
Printed in the United States

A MECHANISM FOR DISLOCATION GENERATION IN SHOCK-WAVE DEFORMATION

Marc A. Meyers
Department of Metallurgical Engineering
South Dakota School of Mines and Technology
Rapid City, South Dakota 57701

(Received August 4, 1977)
(Revised October 3, 1977)

Introduction

Numerous articles describing the changes in structure and mechanical response of metals and alloys induced by shock waves have been published in the past twenty years (1-3). Increases in the concentration of point (4) and line defects (5), formation of twins (6), martensite (7) and precipitates (8) have been observed in the residual structures. Smith (9) proposed the first model accounting for dislocation generation in shock loading. According to this model, a two-dimensional array of dislocations separated the high-density shocked material from the virgin material; the translation of this two-dimensional interface coincided with the shock-front propagation. Aware of the fact that the passage of such an interface would result in undeformed material, Smith (9) hypothesized the presence of sources and sinks of dislocations, moving with the velocity of the shock front. Hornbogen (10), based on the fact that shock-loaded iron (between 7 and 11 GPa) presents a substructure characterized by straight screw dislocations, proposed a modification to Smith's (9) model. Shock loading would induce the formation of loops; the edge components would propagate with the front, basically forming a Smith interface. However, the screw components would stay behind and would therefore be the salient residual feature of the substructure. Cowan (11) suggested that at shock pressures generating shear stresses above the theoretical shear stress of the material a difference in dislocation generation mechanism might be expected. Above this stress, termed by him "supercritical stress," the limitations imposed on dislocation velocity would no longer be valid, and a Smith (9) interface might become possible. No specific mechanism is however proposed by him.

Smith's (9) and Hornbogen's (10) proposals require that the participating dislocations, because they move with the front and at a certain angle, have actually velocities higher than the shock front velocity. The velocity of the shock front is either slightly below (at low pressures) or slightly above (at higher pressures) the longitudinal sound velocity in the material. Therefore transonic and/or supersonic dislocations are involved (12-15). It is the objective of this note to propose a model for dislocation generation in shock-wave deformation that does not require transonic or supersonic dislocation velocities. This model permits the prediction of residual dislocation densities. The calculated dislocation densities are compared with experimental results by Kressel and Brown (16), Trueb (17), and Murr and Kuhlmann-Wilsdorf (18).

Mechanism

The state of deformation induced by shock loading is, by nature, one of uniaxial strain. It should not be confused with other types of plastic waves, as the ones generated for instance in Hopkinson bars. The stress state corresponding to the above deformation is, according to linear elasticity theory, the same for isotropic and cubic materials. The stress state corresponding to the uniaxial strain is a three-dimensional stress; it can be decomposed into a hydrostatic and a deviatoric component. The deviatoric stresses are responsible for plastic deformation and the associated substructure generation. Figure 1 shows an elastic wave traversing a simple cubic lattice along a [110] direction. The compressed region is distorted from cubic to monoclinic; in Figure 1, $d_2 < d_1$ and $\theta_2 < \theta_1$. As the wave amplitude increases and the deviatoric

stresses approach the theoretical shear strength of the crystal, dislocations are generated at the interface. Figure 1 illustrates how the distorted lattice is replaced by the reduced cubic lattice plus interfacial dislocations. The thermodynamic instability of the distorted monoclinic lattice will be the driving energy for its transformation into the reduced cubic lattice; the interfacial dislocations (Smith interface) are the transformation by-product. The uniqueness of the proposed mechanism stems from the fact that the dislocations are homogeneously nucleated at the interface; the classical mechanisms (Frank-Read, Li) do not have to be involved. A simplified calculation for nickel using data extrapolated from Hirth and Lothe (19) shows that the shear stresses for homogeneous dislocation generation correspond to pressures easily achieved by shock loading. The shear stress required for the homogeneous nucleation of a partial dislocation at ambient temperature can be approximated as (19):

$$\frac{\tau_h}{G} \simeq 0.054 \tag{1}$$

τ_h is the shear stress required, and G the shear modulus. For polycrystalline nickel G = 76 GPa (ref. 22, Table 6), and one has:

$$\tau_h \simeq 4.10 \text{ GPa} \tag{2}$$

Equating the maximum shearing stress at the shock front with τ_h, one gets:

$$\tau_{max} = \tau_h \simeq 4.10 \text{ GPa} \tag{3}$$

By proper manipulation of the stress and strain tensors (20), and taking the pressure P as the hydrostatic component of the stress system imposed by shock loading, one obtains:

$$\tau_{max} = \frac{\sigma_1 - \sigma_3}{2} = \frac{E\,\varepsilon_1}{2(1+\nu)} = \frac{3(1-2\nu)}{2(1+\nu)}\,P \tag{4}$$

Where σ_1, σ_3 and ε_1 are principal stresses and strain,and ν is Poisson's ratio. Taking $\nu = 0.305$ (average of three values, Table 5, ref. 22) for nickel, one has:

$$\tau_{max} = 0.45\,P \tag{5}$$

Substituting (5)into (3), one gets:

$$P_{min} = 9.15 \text{ GPa} \tag{6}$$

This is the minimum pressure for homogeneous dislocation generation in nickel. Actually, this pressure should be lower because transient heating will reduce τ_h from the value of 4.10 GPa. The stress to homogeneously nucleate a dislocation is not much lower than the theoretical shear stress of the material. Figure 2(a) shows the dislocation interface and the compressed structure, where the deviatoric stresses were relieved. This is the Smith interface.

The critical difference between the model herein proposed and Smith's (9) model is that the dislocations do not move with the shock front, Figures 2(b) and 2(c). As the wave progresses, the deviatoric stresses reach the critical level, dislocations are again "pinched out" at the front. The process repeats itself periodically, as the wave traverses the material (the periodic changes in deviatoric stresses at the shock front are illustrated in Figure 5). Figure 2(b) shows the Smith interface left behind the front, while the deviatoric stresses elastically distort the lattice. Figure 2(c) shows the front after these deviatoric stresses have reached their critical value; new two-dimensional arrays of dislocations have been generated. The strain constraints are such that contiguous layers of these arrays are composed of dislocations having opposite signs. The important fact to notice is that dislocation generation --and not dislocation motion --is responsible for the accomodation of the deviatoric strains. Consequently, the Orowan equation - - relating strain rate to dislocation velocity - - is not applicable to the shock front.

The dislocations do not maintain, of course, their regular two-dimensional arrays. They reorganize themselves into more stable cinfigurations during the application of the pressure pulse.

Calculated and Experimental Residual Dislocation Densities

In order to verify how realistic the model is, residual dislocation densities were calculated and compared to experimental results reported by Kressel and Brown (16), Trueb (17), and Murr and Kuhlmann-Wilsdorf (18) for nickel. Murr and Kuhlmann-Wilsdorf (18) recently found, for

shock-loaded nickel, that the dislocation cell diameter was inversely proportional to the peak pressure and to the square root of the dislocation density, consistent with the principle of similitude. They also observed that dislocation density was essentially independent of pulse duration, in the 1-6 μs range. The non-dependence of dislocation density on pulse duration points to the fact that dislocations are either generated at the shock front or rarefaction part of the wave. Figure 3 shows a pressure vs. V/V_0 plot for nickel (21), where V and V_0 are the specific volumes at the pressure P and at atmospheric pressure, respectively. Because of the uniaxial strain state, one has:

$$\frac{V}{V_0} = 1-\epsilon_x, \tag{7}$$

where ϵ_x is the uniaxial strain. In the model proposed in the foregoing section, one can assume that all grains have the orientation shown in Figures 1 and 2, as a first approximation. So:

$$1-\epsilon_x = \frac{d_2}{d_1} = \frac{V}{V_0} \tag{8}$$

Table I shows the different values. Assuming that the Burgers vector of each dislocation

TABLE I

Calculation of Dislocation Densities

Pressure (GPa)	$V/V_0 = d_2/d_1$	# of distances d_1 per dislocation doublet	Dislocation Spacing at Front (A)	Calculated Dislocation Density (cm^{-2})
8	0.962	26.32	65.67	1.16×10^{12}
10	0.953	21.28	53.01	1.78×10^{12}
25	0.903	10.31	25.68	7.58×10^{13}
37	0.871	7.75	19.31	1.34×10^{13}
46	0.852	6.76	16.84	1.76×10^{13}
60	0.822	5.62	14.00	2.55×10^{13}
100	0.767	4.35	10.84	4.25×10

is equal to d_1, one can calculate the dislocation spacing, in d_1 units. It can be seen that, as the pressure increases, the dislocation spacing decreases. The lattice parameter for nickel is 3.52 A, yielding d_1 = 4.98 A. This provides the dislocation spacing at the shock front. Multiplying this value by $2d_3$ one obtains the area occupied by one dislocation along the cross-section shown in Figure 2. The distance d_3 between dislocation layers (Figure 2(c)) depends on the rate of build-up of deviatoric stresses in the lattice (Figure 5). For the purpose of these calculations it was assumed equal to the separation between dislocation doublets at the front (Table I). The factor 2 was introduced to account for the fact that, for each mismatch of d_1, two dislocations--one along each of the perpendicular set of (100) planes--are generated. Figure 4 shows a plot of dislocation densities vs. pressure. The calculated values are higher, by more than one order of magnitude, than the experimental ones. In addition to the assumptions used in the model, there are three main reasons for the higher calculated dislocation densities:

a) The mechanism assumed that enough dislocations are formed at the front to reduce the deviatoric stresses to zero. However, it is recognized that the number of dislocations generated should actually be below the calculated one, since the lattice can absorb elastically substantial deviatoric stresses.

b) It is probable that dislocation annihilation can take place during the application of the pressure pulse and at the rarefaction part of the wave, because of the high pressure and transient temperature. The fact that contiguous layers are formed of dislocations at opposite sign (Figure 2(c)) would certainly help annihilation.

c) The model assumed immobile dislocations. In effect, after being generated, the dislocations are impelled towards the front by the stress fields due to the already existing dis-

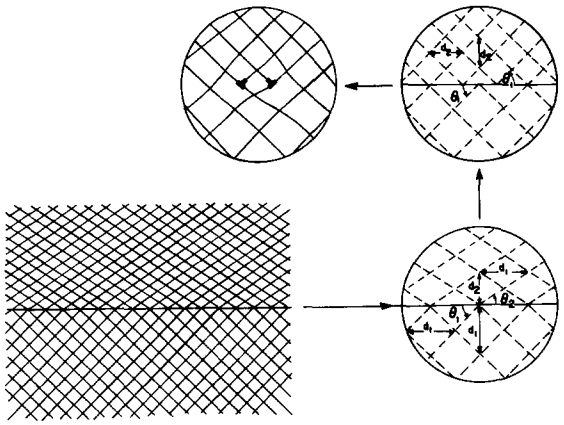

FIG. 1

Schematic representation of how elastic distortion of shocked region is transformed into hydrostatic compression plus dislocation generation (Smith interface (9)).

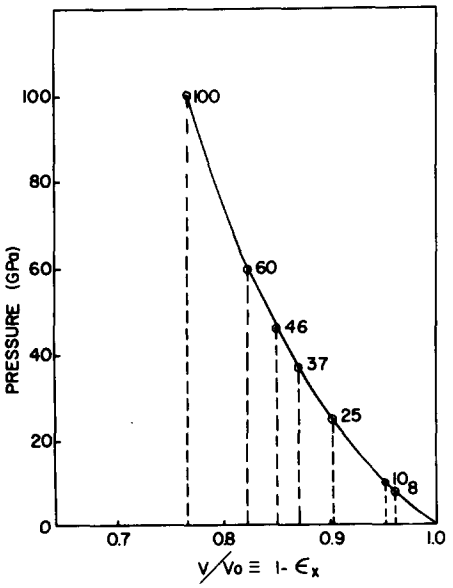

FIG. 3

Pressure vs. specific volume curve for Ni(21).

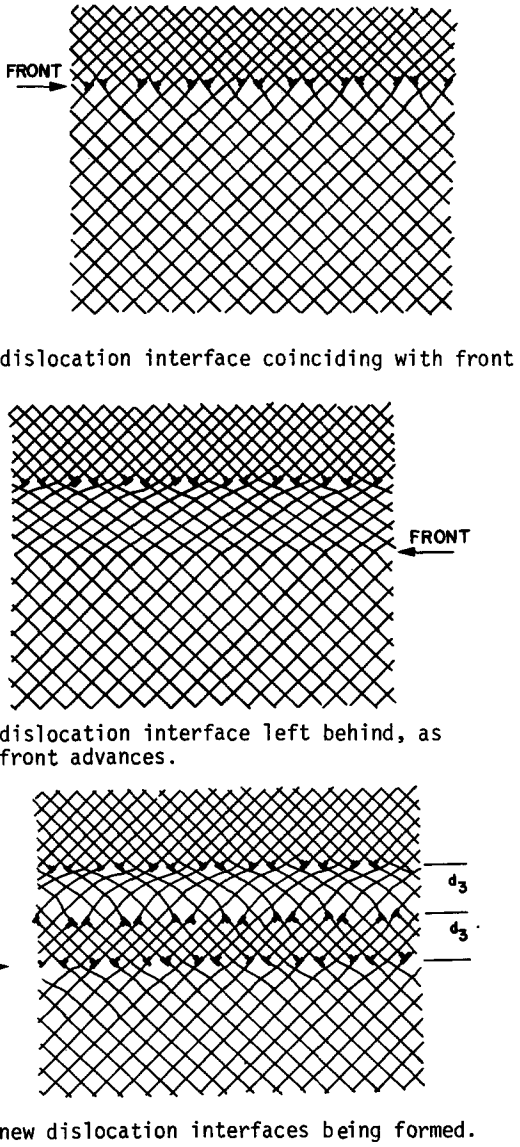

FIG. 2

Proposed Mechanism.

locations (the earlier formed layers). Assuming that their limiting velocity is the shear sound velocity in the compressed medium (higher than the shear wave velocity in the virgin material), they will move at velocities over half of the shock-front velocities; they are therefore able to retard the build-up of deviatoric stresses. The net effect is an increase in d_3 and, consequently, a decrease in the residual dislocation density. Figure 5 shows a plot of the variation of hydrostatic and deviatoric stresses with distance, with and without dislocation movement. While the hydrostatic stress remains constant, the deviatoric stress varies cyclically between zero and the stress required for homogeneous dislocation nucleation.

These three effects will substantially reduce the dislocation densities from the values shown in Figure 4. Arbitrary values could be attributed to them and incorporated into the mechanism,bringing observed and calculated values of Figure 4 to superposition. However, any hypothesis as to the relative efficiency of the aforementioned effects in reducing the overall dislocation density is regarded by the author as speculative, at the present moment.

Lastly, the dislocations, after being generated at the shock front, and having reorganized themselves during the application of the pulse (18), undergo the "decompression". The lattice returns to atmospheric pressure, and the attenuation of the wave will create deviatoric stresses equal, in magnitude, to the ones at the shock front. However, the rate of attenuation of the shock pressure is much lower than its rate of increase, at the front. For example, a 3.2 mm copper driver plate impacting a nickel sample at a velocity of 260 m/sec generates a pressure of 21.2 GPa, a pulse duration of 1.20 μsec, and a rarefaction rate of -52.1 GPa/μsec. Consequently, the pressure is reduced from its peak value to zero in 0.4 μsec. The uniaxial strain ϵx is approximately 0.08; it will yield a maximum shear strain equal to approximately 0.04. The observed residual dislocation density for this pressure is around $7 \times 10^{10} cm^{-2}$. The two main differences between the shock and rarefaction parts of the wave are that the latter encounters an already highly dislocated substructure ($\sim 7 \times 10^{10} cm^{-2}$ at 21.2 GPa) and that the time interval over which it takes place is much larger (0.4 μsec). One could therefore assume that the accomodation of the deviatoric stresses during rarefaction can take place by movement of the existing dislocations. This hypothesis can be tested using Orowan's equation:

$$\gamma = \rho \, b \, \bar{l} \qquad (9)$$

γ is the maximum shear strain, ρ the dislocation density, b the Burgers vector, and $\bar{l}$ the average distance that each dislocation would have to move. For the example under discussion ($\rho = 7 \times 10^{10} cm^{-2}$; b=2.5A; γ=0.04), $\bar{l}$ is equal to 2280 A. This distance is larger than the inter-dislocation spacing (378A, assuming uniform distribution of dislocations). This displacement would have to take place over a time interval of 0.4 μsec; consequently, the average velocity of the dislocations would be 0.57 m/sec. However, it is probable that the mobile dislocation density is much lower than the total dislocation density (this is the case for dislocations locked into cell walls). This would result in an increase in $\bar{l}$. However, a dislocation cannot freely move in a lattice over distances much above the inter-dislocation spacing. Consequently, the deviatoric stresses at the rarefaction part of the wave would not be accomodated entirely by dislocation motion; dislocation generation would be required. It is however thought that the number of dislocations generated at the rarefaction part of the wave is lower than the number generated at the shock front, since part of

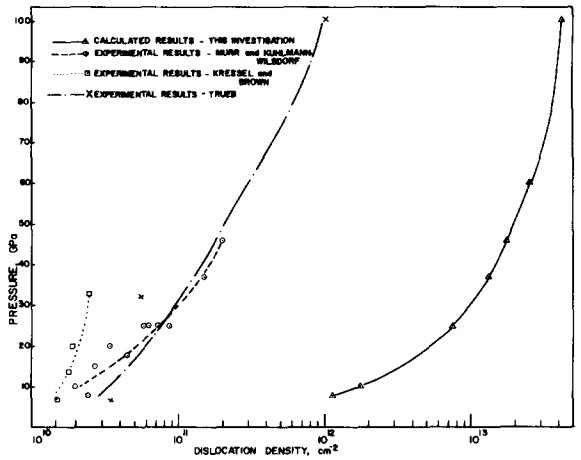

FIG. 4

Experimental and calculated (assuming no dislocation motion, annihilation, and no residual deviatoric stresses) dislocation densities for nickel as a function of shock-loading pressure.

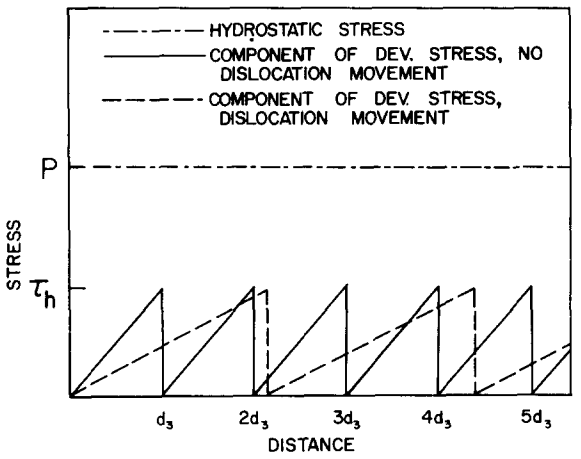

FIG. 5

Effect of dislocation motion on the rate of build-up of deviatoric stresses.

the stresses can be accomodated by dislocation motion. It can be seen from equation (9) and from the pressure dependence of dislocation density that the relative contributions of dislocation generation and dislocation motion at the rarefaction part of the wave depend on pressure.

It should be pointed out that, if a pre-strained metal is shock-loaded, part of the deviatoric stresses at the shock front could be accomodated by the existing dislocations; in this case the number of dislocations that would be generated at the front would be reduced. However, since the steepness of the shock front is much higher than the rarefaction rate--the time interval between zero and maximum pressure is about 10^{-3} μsec (9)--the motion of the existing dislocations would be more restricted than at the rarefaction part of the wave.

Concluding Remarks

A mechanism for the formation of dislocations in shock-wave deformation of metals is proposed. According to the model, dislocations are homogeneously generated at the shock front, once the deviatoric stresses exceed a certain critical value. Contrary to Smith's model (9) however, dislocations are left behind the front. Consequently, dislocation generation, and not dislocation motion accounts for the plastic strains introduced by the shock front. Dislocations can move, and probably do so, but no transonic and/or supersonic velocities are imposed on them. What renders this model attractive, in comparison with previous models, is that it allows a quantitative prediction of residual dislocation densities, Figure 4. The use of appropriate correction factors for dislocation motion, annihilation, and residual deviatoric stresses could bring calculated and experimental results into exact superposition. It is to be noted that this mechanism does not apply to very low pressures, where yielding at the elastic precursor wave accounts for the dislocations produced. It is suggested that the accomodation of deviatoric strains at the rarefaction part of the wave takes place both by the movement of the existing dislocations and by fresh dislocation generation.

Acknowledgements

Support of this investigation by the U. S. Army Research Office (ARO Grant Number DAAG29-76-G-0181) is gratefully acknowledged. Appreciation is extended to Professors D. Kuhlmann-Wilsdorf and L. E. Murr for permission to use their data prior to publication and to Professors L. E. Murr, R. N. Orava, A. Pattnaik, and G. A. Stone for helpful discussions.

References

1. G. E. Dieter, in "Strengthening Mechanisms," ASM, Metals Park, Ohio (1962).
2. Response of Metals to High-Velocity Deformation, AIME, Interscience, N.Y. (1961).
3. Metallurgical Effects at High Strain Rates, AIME, Plenum Press, N.Y. (1973)
4. L. E. Murr, O. T. Inal, and A. A. Morales, Acta Met. 24, 261 (1976).
5. L. E. Murr and J. -Y. Huang, Mat. Sci. and Eng. 19, 115 (1975).
6. D. C. Brillhart, R. J. De Angelis, A. G. Preban, J. B. Cohen, and P. Gordon, Trans. TMS-AIME 239, 836 (1967).
7. L. E. Murr and K. P. Staudhammer, Mat. Sci. and Eng. 20, 35 (1975).
8. C. Stein, Scripta Met. 9, 67 (1975).
9. C. S. Smith, Trans. TMS-AIME 212, 574 (1958).
10. E. Hornbogen, Acta Met. 10, 978 (1960).
11. G. E. Cowan, Trans. TMS-AIME 233, 1120 (1965).
12. J. Weertman, Source cited in ref. 3, p. 319.
13. J. Weertman, Sci. Prog., Oxf. 61, 241 (1974).
14. D. Kuhlmann-Wilsdorf, in "Physical Metallurgy," ed. R. W. Cahn, 2nd edition, Chap. 13, p. 787, North-Holland, Amsterdam (1970).
15. J. Weertman and J. R. Weertman, in "Dislocation Theory: A Treatise", Vol. III, Chap. 8, ed. F. R. N. Nabarro, North-Holland, Amsterdam, in press.
16. H. Kressel and N. Brown, J. Appl. Phys. 38, 1618 (1967).
17. L. Trueb, J. Appl. Phys. 40, 2976 (1969).
18. L. E. Murr and D. Kuhlmann-Wilsdorf, Acta Met., submitted for publication (1977).
19. J. P. Hirth and J. Lothe, Theory of Dislocations, p. 689, McGraw-Hill, N.Y. (1968).
20. G. E. Dieter, Mechanical Metallurgy, Second Edition, pp. 31,44,52,53, McGraw-Hill, N.Y. (1976).
21. R. G. McQueen and S. P. Marsh, J. Appl. Phys. 31, 1253 (1960).
22. R. Hutt, Mat. Sci. and Eng. 29, 55 (1977).